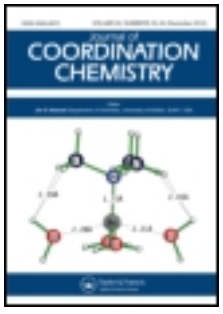

Journal of Coordination Chemistry
Publication details, including instructions for authors and subscription information:
http://www.tandfonline.com/loi/gcoo20

Syntheses, crystal structures, and electrochemical characterizations of two octahedral iron(III) complexes with Schiff base of pyridoxal and aminoguanidine

Mirjana M. Lalović [a], Ljiljana S. Jovanović [a], Ljiljana S. Vojinović-Ješić [a], Vukadin M. Leovac [a], Valerija I. Češljević [a], Marko V. Rodić [a] & Vladimir Divjaković [a]

[a] Faculty of Sciences, University of Novi Sad, Trg Dositeja Obradovića 3, 21000 Novi Sad, Serbia

Accepted author version posted online: 09 Oct 2012.Published online: 23 Oct 2012.

To cite this article: Mirjana M. Lalović, Ljiljana S. Jovanović, Ljiljana S. Vojinović-Ješić, Vukadin M. Leovac, Valerija I. Češljević, Marko V. Rodić & Vladimir Divjaković (2012) Syntheses, crystal structures, and electrochemical characterizations of two octahedral iron(III) complexes with Schiff base of pyridoxal and aminoguanidine, Journal of Coordination Chemistry, 65:23, 4217-4229, DOI: 10.1080/00958972.2012.737916

To link to this article: http://dx.doi.org/10.1080/00958972.2012.737916

Journal of Coordination Chemistry
Vol. 65, No. 23, 10 December 2012, 4217–4229

Syntheses, crystal structures, and electrochemical characterizations of two octahedral iron(III) complexes with Schiff base of pyridoxal and aminoguanidine

MIRJANA M. LALOVIĆ, LJILJANA S. JOVANOVIĆ, LJILJANA S. VOJINOVIĆ-JEŠIĆ, VUKADIN M. LEOVAC*, VALERIJA I. ČEŠLJEVIĆ, MARKO V. RODIĆ and VLADIMIR DIVJAKOVIĆ

Faculty of Sciences, University of Novi Sad, Trg Dositeja Obradovića 3, 21000 Novi Sad, Serbia

(*Received 6 July 2012; in final form 7 September 2012*)

This article presents the synthesis, physico-chemical, in particular voltammetric, characteristics of two iron(III) complexes with pyridoxal aminoguanidine (PLAG), $[Fe(PLAG)Cl_2(H_2O)]Cl$ (**1**) and $[Fe(PLAG)_2](NO_3)_3$ (**2**). As expected, the zwitterion of the chelate ligand is coordinated tridentate through oxygen of phenol and nitrogen atoms of azomethine and imino groups of the aminoguanidine fragment. In both complexes, Fe(III) is distorted octahedral. $[Fe(PLAG)_2](NO_3)_3$ (**2**) is the first bis(ligand) complex with this ligand. Cyclic voltammetric characteristics of the ligand and complexes were studied in DMF in the presence of TBAP or LiCl as supporting electrolytes. The complexes are unstable in this solvent, especially in the presence of an excess of chloride, thus forming several reducible species whose stabilities and behaviors were characterized.

Keywords: Pyridoxal; Aminoguanidine; Fe(III) Complexes; Crystal structure; Electrochemistry

1. Introduction

Due to their significant roles in biochemical processes, pyridoxal and pyridoxal phosphate have been subject of extensive studies [1–4]. In the presence of metal ions pyridoxal can catalyze important metabolic reactions, such as transamination, decarboxylation, and racemization of amino acids [3, 4].

Recently, Schiff bases of pyridoxal, as one of the forms of vitamin B_6, have been studied by both coordination chemists and pharmacologists, as these compounds show good complexing properties and significant biological activities [5, 6].

Since 1950, when its first significant biological activity was proven [7], aminoguanidine has been a research subject. This compound is well-known as an inhibitor of advanced glycation end products formation [7–10], capable of preventing some side effects of cisplatin, i.e. damage of the kidneys [11]. Considering this, it is not surprising

*Corresponding author. Email: vukadin.leovac@dh.uns.ac.rs

ISSN 0095-8972 print/ISSN 1029-0389 online
http://dx.doi.org/10.1080/00958972.2012.737916

that among the Schiff bases of pyridoxal, the one with aminoguanidine (PLAG) occupies a special place, since it has shown significant antioxidant activity and important ability to inhibit advanced glycation [12, 13]. It has been reported that PLAG was more effective than aminoguanidine in the treatment of diabetic complications due to the better nephropathy control and prevention of vitamin B_6 deficiency [13–15]. Considering the biological and medical importance of PLAG, the synthesis and characterization of its metal complexes are of interest.

Only a few metal complexes with PLAG, namely complexes of Cu(II), have been synthesized and structurally characterized [16–18]. However, since both ligand precursors and the ligand itself have significant biological activities, the syntheses and characterizations of other metal complexes with PLAG seem worthwhile.

In this article, we present the syntheses, voltammetric, and structural characterizations of the first two complexes of Fe(III) with PLAG, $[Fe(PLAG)Cl_2(H_2O)]Cl$ (**1**) and $[Fe(PLAG)_2](NO_3)_3$ (**2**).

2. Experimental

2.1. *Materials and physico-chemical measurements*

All chemicals used were commercial products of analytical reagent grade. Elemental analyses (C, H, and N) of air-dried complexes were carried out by standard micromethods. Iron contents in the complexes were determined by chelatometric titration with EDTA, upon their destruction with HNO_3 and H_2SO_4. Melting points were measured on a Nagema melting point microscope *Rapido*. Magnetic susceptibility measurements were conducted at room temperature on an MSB-MKI magnetic susceptibility balance (Sherwood Scientific Ltd., Cambridge). Molar conductivities of freshly prepared 1×10^{-3} mol dm^{-3} solutions were measured on a Janway 4010 conductivity meter. IR spectra were recorded from 4000 to 400 cm^{-1} at room temperature (KBr pellet) on a Thermo Nicolet (NEXUS 670 FTIR) spectrophotometer. UV-Vis spectra of DMF solutions were recorded on a T80 + UV/VIS Spectrometer PG Instruments Ltd. from 270 to 1100 nm. Cyclic voltammetric experiments were carried out on a VOLTALAB PST050 potentiostat with a glassy carbon disc (diameter 3 mm) working electrode, Pt wire counter electrode, and a saturated calomel electrode as reference. All potentials are reported against this electrode. The measurements were done in analytical grade *N*,*N*-dimethylformamide (DMF) which was vacuum distilled after prior drying on molecular sieves. Supporting electrolyte was 0.1 mol L^{-1} tetrabutylammonium perchlorate (TBAP). Experiments were carried out in an inert atmosphere provided by bubbling nitrogen.

2.2. *Synthesis of the ligand*

PLAG was obtained by the partly simplified procedure described [12]. Aminoguanidine hydrogencarbonate (0.68 g, 5.0 mmol) was dissolved in warm H_2O (10 mL), to which a warm solution of pyridoxal hydrochloride (1.00 g, 5.0 mmol) in H_2O (5 mL) was added. To this solution was added $Na_2CO_3 \cdot 10H_2O$ (0.71 g, 2.5 mmol) dissolved in H_2O (10 mL), and the mixture was mildly heated for a couple of minutes. The obtained

solution was left at room temperature for about 20 h, after which yellow crystals were separated by filtration and washed with EtOH and Et_2O. Yield: 95%; m.p. = 152°C. Anal. Calcd for $C_9H_{13}N_5O_2$ (%): C, 48.29; H, 5.87; N, 31.37. Found: C, 47.91; H, 5.11; N, 31.18. Λ_M (MeOH): 3.7 S cm^2 mol^{-1}. IR data (cm^{-1}): 3107(w), 1697(m), 1631(m), 1531(m), 1437(m), 1390(s), 1369(s), 1290(m), 1250(w), 1216(m), 1170(w), 1115(w), 1099(m), 991(m), 946(w), 925(w), 747(m), 641(m), 610(m), 551(w), 522(w), 450(w). UV-Vis (DMF) [λ_{max}/nm (log ε/(mol L^{-1})$^{-1}$ cm^{-1})]: 313 (4.12), 332 (3.60), 350 (4.04), 369 (4.21).

2.3. *Synthesis of [Fe(PLAG)Cl$_2$(H$_2$O)]Cl (1)*

To a warm MeOH (10 mL) solution of PLAG (0.11 g, 0.5 mmol) was added $FeCl_3 \cdot 6H_2O$ (0.13 g, 0.5 mmol). The resulting dark-red solution was mildly heated and left at room temperature. After 5 days, the partially dry residue was poured over with acetone and filtered after 30 min, the flickering dark-red single crystals were separated by filtration and washed with acetone and Et_2O. Yield: 65%; m.p. = 238°C. Anal. Calcd for $C_9H_{15}Cl_3FeN_5O_3$ (%): Fe, 13.84; C, 26.76; H, 3.72; N, 17.35. Found: Fe, 13.51; C, 27.58; H, 4.11; N, 17.34. Λ_M (H_2O, MeOH): 415; 148 S cm^2 mol^{-1}. μ_{eff} = 2.60 BM. IR data (cm^{-1}): 3383(w), 3309(m), 3242(w), 3085(w), 1649(s), 1590(m), 1553(s), 1499(w), 1428(m), 1371(m), 1330(w), 1255(w), 1215(w), 1172(m), 1069(m), 1025(m), 813(m), 745(m), 527(w), 412(w). UV-Vis (DMF) [λ_{max}/nm (log ε/(mol L^{-1})$^{-1}$ cm^{-1})]: 280 (4.20), 340 (4.02), 441sh (3.84), 534sh (3.74) (sh – shoulder).

2.4. *Synthesis of [Fe(PLAG)$_2$](NO$_3$)$_3$ (2)*

The mixture of PLAG (0.11 g, 0.5 mmol) and $Fe(NO_3)_3 \cdot 9H_2O$ (0.10 g, 0.25 mmol) was dissolved in warm EtOH (7 mL). After 20 h, from the dark-red solution, dark red rod-shaped single crystals were filtered off and washed with EtOH and Et_2O. Yield: 11.7%; m.p. > 350°C. Anal. Calcd for $C_{18}H_{26}FeN_{13}O_{13}$ (%): Fe, 8.11; C, 31.41; H, 3.81; N, 26.45. Found: Fe, 7.98; C, 30.86; H, 3.73; N, 26.10. Λ_M (H_2O, MeOH): 340; 240 S cm^2 mol^{-1}. μ_{eff} = 2.13 BM. IR data (cm^{-1}): 3435(w), 3332(w), 3274(m), 2859(w), 1641(s), 1587(m), 1553(m), 1504(m), 1384(vs), 1327(m), 1247(m), 1164(m), 1067(m), 1030(m), 979(w), 748(w), 621(w), 457(w). UV-Vis (DMF) [λ_{max}/nm (log ε/(mol L^{-1})$^{-1}$ cm^{-1})]: 283 (4.50), 340 (4.21), 442sh (3.48), 534sh (3.11).

2.5. *Single-crystal X-ray experiment*

Single crystals of **1** and **2** were selected and glued on glass fibers. Diffraction measurements were performed on a Gemini S diffractometer (Agilent Technologies) equipped with a Sapphire CCD detector. The crystal to detector distance was 45 mm and graphite monochromated Mo-Kα (0.71073 Å) radiation was used. The data were reduced using the *CrysAlisPRO* (Agilent Technologies). A semi-empirical absorption correction was applied and the data were corrected for Lorentz, polarization, and background effects. The structures were solved by direct methods using *SIR92* [19] and refined by full-matrix least-squares on F^2 using *SHELXL-97* [20]. All non-H atoms were refined with anisotropic displacement parameters. The positions of all hydrogen atoms

were found by inspection of ΔF maps. In the final stage of refinement, hydrogen atoms belonging to ligand were positioned geometrically (N–H = 0.86; C–H = 0.93 and 0.97 Å for CH and CH_3, respectively) and refined using a riding model with U_{iso} equal to 1.2 (for NH and CH) and 1.5 (for CH_3) U_{eq} of parent atoms. Positions of hydrogen atoms corresponding to H_2O in **1** were refined with restrained O–H distances (O–H = 0.82 Å) with U_{iso} equal to 1.5 U_{eq} of oxygen. The programs used to prepare material for publication are *WINGX* [21] and *PLATON* [22]. Crystal data and refinement parameters are listed in table 1.

3. Results and discussion

3.1. *Synthesis and physico-chemical properties of the complexes*

Dark red single crystals of **1** and **2** were obtained by reaction of warm alcohol solutions of Fe(III) salts and ligand in molar ratios of 1 : 1 and 1 : 2. The complexes are crystalline substances stable in air and at higher temperatures. They are soluble in H_2O, MeOH, and DMF, and less soluble in EtOH and acetone.

The molar conductivity of **1** in water corresponds to an electrolyte of 3 : 1 type [23], which indicates the displacement of both coordinated chlorides with water. In contrast to that, the somewhat lower value of the molar conductivity of the MeOH solution

Table 1. Crystallographic data for **1** and **2**.

Crystallographic data	**1**	**2**
Empirical formula	$C_9H_{15}Cl_3FeN_5O_3$	$C_{18}H_{26}FeN_{13}O_{13}$
Formula weight	403.46	688.37
Temperature (K)	298(2)	298(2)
Wavelength (Å)	0.71073	0.71073
Crystal system	Orthorhombic	Monoclinic
Space group	$P\ 2_12_12_1$	$C\ 2/c$
Unit cell dimensions (Å)		
a	7.35121(18)	28.8516(19)
b	8.4892(2)	9.4411(6)
c	25.0469(8)	22.2743(15)
β		113.397(8)°
Volume (Å^3), Z	1563.07(7), 4	5568.4(6), 8
Calculated density (g cm^{-3})	1.714	1.642
Absorption coefficient (mm^{-1})	1.493	0.631
$F(000)$	820	2840
Crystal size (mm^3)	$0.15 \times 0.11 \times 0.05$	$0.12 \times 0.09 \times 0.03$
Color/habit	Dark red/prism	Black/prism
θ range for data collection (°)	3.21–25.00	3.52–24.99
Index ranges	$-8 \le h \le 8$; $-6 \le k \le 10$; $-23 \le l \le 29$	$-34 \le h \le 30$; $-6 \le k \le 11$; $-26 \le l \le 26$
Reflection collected	4431	9981
Unique reflection	2699 ($R_{int} = 0.0178$)	4883 ($R_{int} = 0.0226$)
Reflections with $I > 2\sigma I_o$	2343	3485
Refinement methods	Full-matrix least-squares on F^2	Full-matrix least-squares on F^2
Data/restraints/parameters	2699/0/198	3485/0/410
Goodness-of-fit on F^2	0.955	1.000
Final R indices [$F_o > 4\sigma F_o$]	$R_1 = 0.0279$	$R_1 = 0.0492$
R indices (all data)	$R_1 = 0.0346$, $wR_2 = 0.0596$	$R_1 = 0.0696$, $wR_2 = 0.1448$

($148\,S\,cm^2\,mol^{-1}$) suggests a partial replacement of these ions with MeOH. The conductivity of aqueous solution of **2** is in accord with its coordination formula, whereas the conductivity of its MeOH solution is somewhat lower than the value for 3 : 1 electrolytes [23]. The observed decrease of conductivity may be due to lower mobility of the large complex cation, as well as to its partial association with NO_3^-.

Effective magnetic moments indicate that the complexes are low spin, which can lead to the conclusion that in the isolated complexes PLAG behaves as a strong ligand. In these complexes, the ligand is coordinated in its neutral form, as a tridentate chelate, as shown by single-crystal X-ray analysis (*vide infra*). The ONN coordination indicates shift of the corresponding IR bands in spectra of the complexes with respect to those in the free ligand. Thus, IR spectra of the ligand and complexes, apart from certain similarities, show differences too. Indication of coordination of oxygen of the deprotonated phenolic OH is the shift of ν(C–O) from $1290\,cm^{-1}$ in the ligand spectrum to $\approx 1330\,cm^{-1}$ in spectra of the complexes [16–18].

Strong bands at $1649\,cm^{-1}$ (**1**) and $1641\,cm^{-1}$ (**2**), belonging to ν(C=N) of the azomethine, shift upon coordination to lower energy compared to the ligand ($1697\,cm^{-1}$) [16–18].

The band that may be ascribed to vibrations of the guanido group, in the ligand spectrum at $1631\,cm^{-1}$ [16], shows a negative shift of $\approx 40\,cm^{-1}$ in spectra of **1** and **2**.

Broad bands of low intensity at $3100–2700\,cm^{-1}$ in spectra of both PLAG and its complexes may be ascribed to $\nu(NH^+)$ of the zwitterionic PL moiety [16–18], formed by migration of hydrogen from the phenolic OH to nitrogen of the PL residue.

Finally, in the IR spectrum of **2**, there is an additional band at $1384\,cm^{-1}$, of a very strong intensity, corresponding to vibrations of non-coordinated NO_3^- [24].

3.2. *Electronic spectra*

Electronic spectra were taken in DMF from 270 to 1000 nm. In the ligand spectrum there are two "doublet-like" bands, one at 313 and 332 nm, the other at 350 and 369 nm. On the basis of previous results and of the log ε values, these bands could be ascribed to $\pi \rightarrow \pi^*$ and $n \rightarrow \pi^*$ transitions of both pyridoxal and aminoguanidine [18, 25]. Addition of protons results in better differentiation of absorption bands which are alike from separate processes on pyridoxal (~285 nm) and aminoguanidine (~340 nm) moieties. Similar situation arises for spectra of both Fe(III) complexes where condensation effects on absorptions are less than on PLAG alone. Thus, the band at ~280 nm can be ascribed to pyridoxal, the other at ~340 nm is located at the aminoguanidine. The other two bands in the spectra of complexes which appear as shoulders on higher wavelengths side belong to charge transfer. Finally, d–d bands cannot be observed in the complexes as frequently observed for Fe(III) [26] due to their weakness and possible masking effects of charge-transfer bands.

3.3. *Crystal structures of 1 and 2*

Molecular structures of the complexes are shown in figures 1 and 2, while lengths and angles of selected bonds are listed in table 2.

A common feature of both complexes is that Fe(III) is situated in a deformed octahedron. Complex **1** has tridentate coordination of the chelate ligand and one

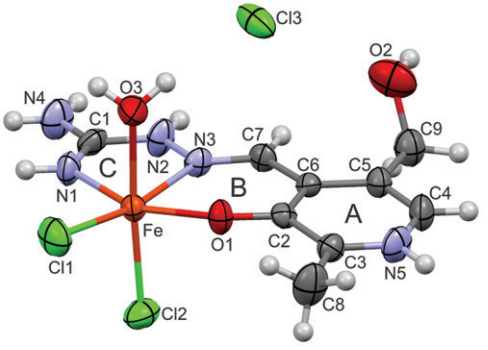

Figure 1. The molecular structure and atom-labeling scheme of **1**.

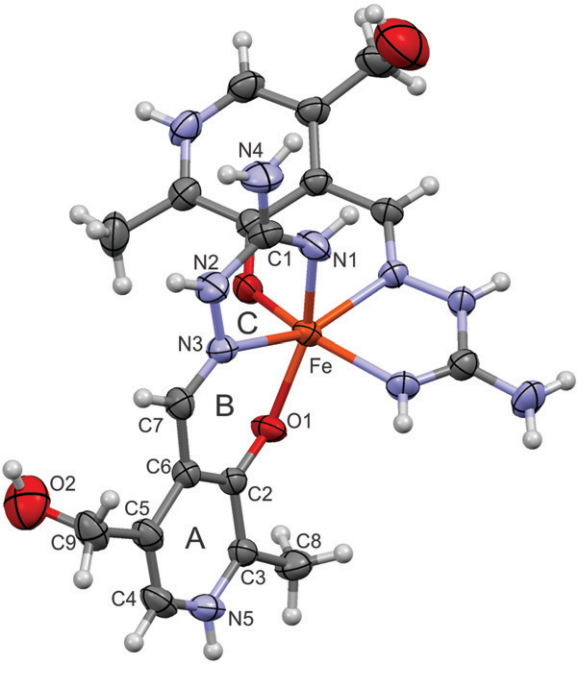

Figure 2. The molecular structure and atom-labeling scheme of the complex cation of **2**.

chloride in the equatorial plane, with the other chloride and one water axial (*cis*-Cl-isomer). In **2**, the tridentate coordination involves two meridional ligands (*mer*-isomer). The positive charge of the complex cations is neutralized by one chloride and three nitrates. In both complexes, there are numerous hydrogen bonds.

PLAG is a tridentate ONN ligand coordinated in the neutral, zwitterionic form through oxygen of the deprotonated OH and nitrogen of azomethine and imino groups of the aminoguanidine fragment. In this way, two metallocycles are formed, one six-membered (pyridoxilidene; ring B) and one five-membered (aminoguanidine; ring C).

In both complexes, Ar–phenolic(O) (C2–O1) (1.295 Å, **1**, and 1.290(3) and 1.305(4) Å, **2**) is significantly shorter than a single C–O bond (1.43 Å) [27], a consequence of

Table 2. Selected bond lengths (Å) and angles (°) for **1** and **2**.

1			
Fe–O1	1.942(2)	N2–N3	1.358(4)
Fe–N1	2.054(3)	N3–C7	1.283(4)
Fe–N3	2.210(2)	C2–O1	1.295(3)
Fe–O3	2.120(3)	N1–Fe–N3	73.8(1)
Fe–Cl1	2.2802(9)	O3–Fe–Cl2	176.11(8)
Fe–Cl2	2.3044(9)	O1–Fe–N3	81.36(9)
C1–N1	1.290(5)	O1–Fe–N1	154.1(1)
C1–N4	1.325(4)	C3–N5–C4	124.9(3)
C1–N2	1.355(4)		
2			
Fe–O1	1.946(3)	Fe–O1A	1.931(3)
Fe–N1	2.029(4)	Fe–N1A	2.028(3)
Fe–N3	2.221 l(3)	Fe–N3A	2.204(2)
C1–N1	1.289(5)	C1A–N1A	1.284(4)
C1–N4	1.328(6)	C1A–N4A	1.343(5)
C1–N2	1.384(5)	C1A–N2A	1.360(4)
N2–N3	1.375(5)	N2A–N3A	1.360(4)
N3–C7	1.284(4)	N3A–C7A	1.287(4)
C2–O1	1.290(3)	C2A–O1A	1.305(4)
N6–O3	1.226(5)	N7–O7	1.257(6)
N6–O4	1.242(5)	N7–O8	1.232(5)
N6–O5	1.252(4)	O1–Fe–N1	153.0(1)
N8–O9	1.232(6)	O1A–Fe–N1A	144.3(1)
N8–O10	1.219(6)	N3–Fe–N3A	156.4(1)
N8–O11	1.199(5)	C3–N5–C4	124.3(3)
N7–O6	1.251(5)	C3A–N5A–C4A	124.7(4)

displacement of the electron density from the pyridine ring of the PL residue toward O1, which, due to participation in coordination, becomes electron deficient. The C1–N2 and C1–N4 lengths of guanido group in both complexes are longer than double bonds but shorter than single C–N bonds, due to their delocalization. However, C1–N1 and C7–N3 lengths have values characteristic of a delocalized double bond. The angle between pyridine nitrogen and neighboring carbons in **1** is 124.9(3)°, and in **2** 124.3(3) and 124.7(4)°, characteristic of a protonated nitrogen [17, 28], proving that pyridoxal is in its zwitterionic form.

Fe(III) is situated in a deformed octahedral surrounding, indicated for **1** by values of the *trans*-angles N3–Fe–Cl1 and N1–Fe–O1 (169.44(7)° and 154.1(1)°, respectively), differing significantly from 180°, whereas the value of the O3–Fe–Cl2 angle is 176.11(8)°. In contrast in **2**, all three relevant angles, N1–Fe–O1, N3–Fe–N3A, and N1A–Fe–O1A, have values significantly lower than the theoretical, 153.0(1), 156.4(1), and 144.3(1)°. Fe(III) in **1** is slightly shifted from the equatorial plane of the coordination polyhedron toward the axial Cl^- by 0.153(3) Å, while in **2** it is coplanar (within the limits of experimental error) with the O1/N3/N1/N3A plane forming the equatorial plane of the octahedron.

Lengths of metal–ligand bonds are 1.942(2)–2.210(2) Å for **1** and 1.931(3)–2.211(3) Å for **2**. Because of the negative charge on O1, a consequence of the zwitterionic form of the ligand, it forms a shorter bond with Fe(III) than the two N-ligators. This was reported in previously characterized complexes with this ligand [16–18], and is typical of the coordination chemistry of PLAG. The Cu–N3 distance in both complexes is longer than the length of the Cu–N1 bond, which can be explained by the fact that the

azomethine is a weaker base than the imino group of aminoguanidine [29]. The axial chloride in **1** is more distant from the equatorial one (by 2.3044(9) and 2.2802(9) Å, respectively).

Because of the conjugated double bonds in the ligand, one could expect that the ligand would be planar. However, due to the formation of metallocycles, there is deviation from planarity, best seen from values of the dihedral angles between the mean plane of the rings A and C, 6.32° for **1** and 17.84 and 21.50° for **2**. Values of the dihedral angles between the mean planes of rings A and B, and rings B and C are 7.61 and 1.69° in **1**, but in **2**, these values are somewhat larger, 10.20 and 8.45° for the one molecule and 11.75 and 15.63° for the other. In **1**, rings A and C are planar, with the largest deviations for C6 (0.026 Å) and N1 (0.030 Å), whereas ring B has a conformation between the screw-boat and envelope, with puckering parameters $\theta = 60.1(11)^\circ$ and $\varphi = 42.2(11)^\circ$. In **2**, A, A1, and C1 rings are planar, with the largest deviation for C6 (0.020 Å), C6A (0.012 Å), and N2A (0.034 Å). Ring B has screw-boat conformation, ring B1 is of envelope conformation, and ring C is a half-chair conformation. The hydroxyl of the PL residue is synclinal with respect to C6 (τ[C6/C5/C9/O2] = 62.43(4)° for **1** and τ[C6/C5/C9/O2] = 77.5(5)° and τ[C6/C5/C9/O2] = 62.5(6)° for **2**), reducing the steric strain and bringing the groups to positions suitable for formation of hydrogen bonds.

Geometric parameters of nitrates in **2** are expected. The shortest bond in NO_3^- is N8–O11, which can be explained by O11 not being included in formation of hydrogen bonds.

The crystal lattices of both complexes are stabilized by an extended hydrogen-bond network. All potential H-donors of the coordinated ligand are involved in formation of H-bonds with chloride (**1**) and oxygen of NO_3^- (**2**), with the exception of N1 in **1**. In both complexes, the zwitterionic form of PL is confirmed by the existence of H-bonds between nitrogen of pyridoxal and the corresponding H-acceptors (table 3).

The packing of the structural units of **1** is shown in figure 3, where there are two CAC zones parallel to the *bc*-plane centered at $z = 1/4$ and $z = 3/4$. The anionic layer is sandwiched between two cationic layers. Cations within the cationic layer are bonded only by N5–H5···Cl2, while the other hydrogen bonds appear only between cationic and anionic layers, since they include Cl^- counterions as an H-acceptor. Linking of zones by hydrogen bonds is not observed.

The packing of the structural units in **2** is shown in figure 4, in which the expanded network of intermolecular H-bonds is visible.

3.4. *Electrochemistry*

The ligand in its neutral form and both Fe(III) complexes were studied in DMF in the presence of TBAP and LiCl electrolyte. The latter was chosen because of the known affinity of Fe(III) toward Cl^- [6, 30–32].

3.4.1. Perchlorate media. The cyclic voltammograms of PLAG were compared with those of its mono- and double-protonated forms [18]. As for PLAG, there are no reduction signals until −1.75 V, where $1\text{-}e^-$ reduction peak ($\Delta E/\Delta \log v = -20$ mV/decade, $I_p/c\ v^{1/2} \sim const$) can be observed. The mono- and di-protonated forms display peaks at −1.0 V and at −0.75 and −1.0 V, respectively. At the far negative potentials

Table 3. Hydrogen-bonding parameters for **1** and **2**.

Complex	*D*–H···*A*	H···*A*	*D*···*A*	∠*D*–H···*A*
1	O3–H3B···Cl3	2.22(4)	3.035(3)	159(4)
	O2–H2···Cl3^{i}	2.44	3.232(3)	161
	N2–H2N···Cl3^{ii}	2.42	3.231(3)	158
	O3–H3A···Cl3^{iii}	2.25(4)	3.073(3)	173(4)
	N4–H4A···Cl3^{iv}	2.37	3.211(3)	165
	N5–H5···Cl2^{v}	2.46	3.149(3)	137
2	N1–H1···O7	2.57	3.320(6)	146
	N1–H1···O8	2.24	3.054(5)	157
	N2–H2···O4^{vi}	2.08	2.789(4)	139
	N2–H2···O5^{vi}	2.48	3.230(5)	147
	N4–H4A···O7	2.55	3.306(6)	147
	N4–H4B···O5^{vi}	2.35	3.159(5)	156
	N5–H5···O9^{vii}	2.29	3.032(5)	145
	N5–H5···O10^{vii}	2.05	2.862(7)	157
	O2–H2B···O5^{viii}	2.02	2.832(6)	172
	N1A–H1A···O4	2.20	3.025(5)	162
	N4A–H4A1···O5^{ix}	2.54	3.141(5)	127
	N4A–H4A2···O6^{x}	2.10	2.927(6)	162
	O2A–H2A···O8^{xi}	2.40	3.146(6)	152
	N2A–H2A1···O6^{x}	2.57	3.259(5)	137
	N2A–H2A1···O7^{x}	2.05	2.893(5)	165
	N5A–H5A···O9^{viii}	2.01	2.829(5)	160

Symmetry transformations: ^{i} $-1+x,y,z$; ^{ii} $-x,-1/2+y,3/2-z$; ^{iii} $1-x,-1/2+y,3/2-z$; ^{iv} $x,-1+y,z$; ^{v} $x,1+y,z$; ^{vi} $1-x,1-y,1-z$; ^{vii} $1-x,y,1/2-z$; ^{viii} $x,-1+y,z$; ^{ix} $1-x,2-y,1-z$; ^{x} $1/2-x,1/2+y,1/2-z$; ^{xi} $1/2-x,-1/2+y,1/2-z$.

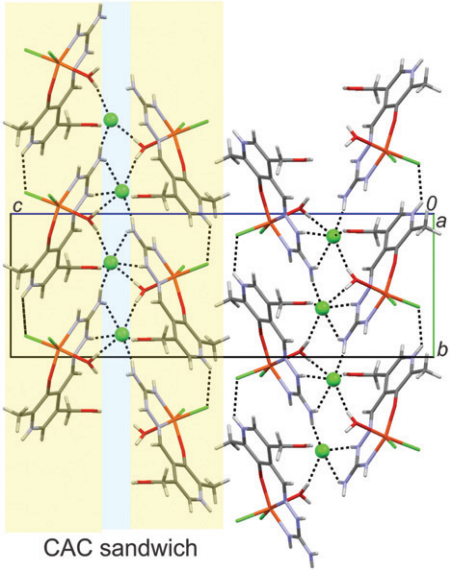

Figure 3. Crystal packing diagram of **1** viewed perpendicular to the *bc*-plane.

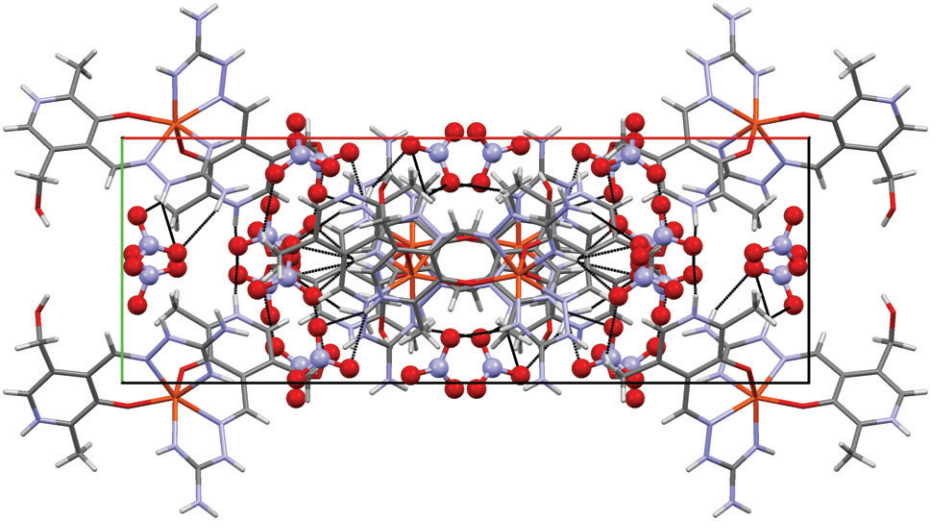

Figure 4. Crystal packing diagram of **2** viewed perpendicular to the *ab*-plane.

(<2.3 V) there is an irreversible multielectron peak corresponding to reduction of imino, as observed earlier [18]. Oxidation for all ligand forms take place in the range +0.7 V to +1.5 V, where up to three irreversible peaks with chemical complications are observed.

The voltammograms of the complexes in perchlorate media are similar to those of analogous Fe(III) complexes with pyridoxal semi-, thiosemi-, and S-methylisothiosemicarbazones [6, 32]. The two voltammograms shown in "Supplementary material" reveal the complexity of solution equilibria and the differences in stabilities of the two complexes. A striking similarity of these voltammograms is that both complexes in solution form several reducible species. Thus, for **2**, only one well-shaped, one-electron reduction peak at −0.5 V is observed, which can be ascribed to reduction of $[Fe(PLAG)_2]^{3+}$. The other peaks at more positive potentials belong to mixed Fe(III)–DMF–ClO_4^- species. In contrast, small amounts of Cl^- greatly affect the complex equilibria in the solution. The ligand-exchange reaction Cl–DMF for Fe(III) complexes was reported [6, 30–34]. Thus, for **1**, three equivalents of Cl^- from the original compound stabilize the species at about 0.0 and −0.25 V. Since the third peak at −0.5 V coincides with the main peak in **2** (Supplementary material), we believe that in both cases it is $[Fe(PLAG)_2]^{3+}$. The mechanism of formation of this species in solutions of the mono(ligand) **1** is discussed in section 3.4.2.

To obtain insight into the Fe(III)–PLAG–Cl^- equilibria we performed successive addition of Cl^- (LiCl) starting from 1 : 1 to 1 : 20 ratio for both complexes. An illustration of the Cl^- effect on the cyclic voltammogram of **1** is shown in "Supplementary material." The two pairs of one-electron peaks, I/I′, and II/II′, are visible in the voltammograms obtained in the presence of excess LiCl. While the potential of II/II′shifts negative, the peak I′ prevails from the two close peaks in TBAP and shifts negative. From the negative shifts of E_p *versus* $[Cl^-]$, ranging from about −150 to −180 mV/decade for $[Cl^-] < 10^{-2}$ mol L^{-1} and diminishing to less than −60 mV/decade for higher $[Cl^-]$, we judge complex equilibria following the electrode processes.

Table 4. Voltammetric characteristics of **1** and **2** in DMF (0.1 mol L^{-1} LiCl) at $v = 0.1$ V s^{-1}.

Complex	$E_p(I)^a$	ΔE_p^b	$E_p(II)$	$I_p^c(I)/c\ v^{1/2}$	$I_p^c(II)/c\ v^{1/2}$
1	−0.070	79	−0.373	34.2	21.7
2	−0.062	74	−0.370	11.0	30.2

[a]Peak potentials (V). [b]$E_p(I') - E_p(I)$ (mV). [c]Peak current function (μA (mmol L^{-1})$^{-1}$ (V s^{-1})$^{-1/2}$).

3.4.2. Chloride media. Cyclic voltammograms for both complexes in LiCl are shown in "Supplementary material." The pairs of peaks, I/I′ and II/II′, are present in both voltammograms, but in different ratios. The third, small peak at −0.6 V could be ascribed to a $[Fe(PLAG)_2]^{3+}\cdots Cl^-$ pair. On the basis of previous results [6, 30–34], the peaks I/I′ belong to the reduction/oxidation of the $[FeCl_4]^-/[FeCl_2]$. Formation of $[Fe(PLAG)_2]^{3+}\cdots Cl^-$ in **1** is a consequence of considerable amounts of free PLAG with $[Fe(PLAG)Cl_3]$. Logically, II/II′ are from the mono(ligand) species of probable composition $[Fe(PLAG)Cl_3]$. Thus, in DMF solutions of **1** and **2** in the presence of LiCl, complex equilibria are established between $[FeCl_4]^-$, $[Fe(PLAG)Cl_3]$, $[Fe(PLAG)_2]^{3+}\cdots Cl^-$ and PLAG. On the basis of the corresponding peak currents it might be supposed that in solutions of **1** about 50% of all Fe(III) species are in the form of $[FeCl_4]^-$, while in **2** it is only 20%.

An interesting feature of the cyclic voltammogram is an obvious increase of peak I′ current in the reverse scan, compared to the initial peak I. This is a consequence of a slow chemical reaction of PLAG release, following reduction at peak II. Thus, the process at peaks II/II′ might be characterized in the following way:

$$\text{II/II}'\ [Fe(PLAG)Cl_3] + e^- \leftrightarrow [Fe(PLAG)Cl_3]^-,$$
$$[Fe(PLAG)Cl_3]^- \rightarrow [FeCl_2] + PLAG + Cl^-,$$
$$\text{I/I}'\ [FeCl_2] + 2Cl^- - e^- \leftrightarrow [FeCl_4]^-.$$

A similar behavior was reported for a series of Fe(III) complexes with thiosemicarbazone-based Schiff bases under the same experimental conditions [6, 30–33].

The peak potentials and current functions are given in table 4. Potentials of II′ are not discernible at this v and are not reported. However, at 1000 mV s^{-1}, where effects of the following chemical reactions are diminished, both II′/II and I′/I behave quasi-reversibly, with ΔE_p 88 and 82 mV, respectively. Peak currents show the distribution of particular species in solution, domination of $[FeCl_4]^-$ in **1**, and $[Fe(PLAG)Cl_3]$ in **2**. In both solutions the bis(ligand) complex $[Fe(PLAG)_2]^{3+}\cdots Cl$ is present only in "residual" amounts, 10% (**1**) and 20% (**2**).

3.4.3. Addition of H^+. To study the effects of protons on species present in solutions of both complexes in chloride medium, we added up to four equivalents of H^+ (as $HClO_4$)/PLAG in successive steps. The protonation can be followed by the disappearance of particular peaks (Supplementary material). The complexes proved to be sensitive to protons in the order −0.6 V → peaks II/II′ → peaks I/I′. By comparing particular peak currents it is possible not only to follow the protonation course, but also to evaluate the composition of the starting solution. After addition of $1H^+$/PLAG to **1**, the peak I doubles its height, indicating about 50% of the initial complex was $[FeCl_4]^-$

(the other half was mainly [Fe(PLAG)Cl_3]). For **2**, the current is finally about 10 times higher, which means that $[FeCl_4]^-$ was initially present at only 10%. The new peak observed in the voltammogram is characteristic of ligand protonated with one proton [18]. Further protonation follows the course of the ligand itself.

The studied Fe(III) compounds exhibit voltammetric behavior similar to that which has already been described, involving complex solution equilibria and electrode processes accompanied by chemical reactions.

4. Conclusion

The article is concerned with the synthesis, X-ray crystallographical and electrochemical characterization of two complexes of Fe(III) with biologically relevant Schiff-base PLAG, [Fe(PLAG)$Cl_2(H_2O)$]Cl (**1**) and [Fe$(PLAG)_2$]$(NO_3)_3$ (**2**) as the first complexes of PLAG with metal other than copper. In both complexes, PLAG is coordinated in the usual tridentate manner, i.e. through oxygen of phenol and nitrogen atoms of azomethine and imino groups of the aminoguanidine fragment. Electrochemical data in DMF in the presence of excess chloride point to instability of reacting species. The results presented, as well as those obtained earlier [35–38] reporting Fe(III) complexes with Schiff bases of different denticity, indicate that this field deserves further investigation.

Supplementary material

CCDC-855935 (**1**) and 855607 (**2**) contain the supplementary crystallographic data. These data can be obtained free of charge from The Cambridge Crystallographic Data Centre *via* www.ccdc.cam.ac.uk/data_request/cif. Supplementary data associated with this article can be found in the online version.

Acknowledgments

This work was supported by the Ministry of Education and Science of the Republic of Serbia (Grant No. 172014).

References

[1] S. Sharif, D.R. Powell, D. Schagen, T. Steiner, M.D. Toney, E. Fogle, H. Limbch. *Acta Cryst*., **B62**, 480 (2006).
[2] D. Dolphin. In *Vitamin B-6 Pyridoxal Phosphate: Chemical, Biochemical and Medical Aspects, Part A*, R. Poulson, O. Avramovic (Eds), pp. 497–544, Wiley, New York (1986).
[3] R.H. Holm. In *Complexes of Vitamin B6 in Inorganic Biochemistry*, G.B. Eichhorn (Ed.), pp. 599–602, Elsevier, Amsterdam (1975).
[4] K. Aoki, H. Yamazaki. *J. Chem. Soc., Chem. Commun*., 363 (1980).

[5] J.T. Wrobleski, G.J. Long. *Inorg. Chem.*, **16**, 2752 (1977).
[6] V.M. Leovac, V.S. Jevtović, Lj.S. Jovanović, G.A. Bogdanović. *J. Serb. Chem. Soc.*, **70**, 393 (2005).
[7] B.-O. Nilsson. *Inflamm. Res.*, **48**, 509 (1999).
[8] C. Scaccini, G. Chiesa, I. Jialal. *J. Lipid Res.*, **35**, 1085 (1994).
[9] P.C. Burcham, L.M. Kaminskas, F.R. Fontaine, D.R. Peterson, S.M. Pyke. *Toxicology*, **181–182**, 229 (2002).
[10] I. Jedidi, P. Therond, S. Zarev, C. Cosson, M. Couturier, C. Massot, D. Jore, M. Gardès-Albert, A. Legrand, D. Bonnefont-Rousselot. *Biochemistry*, **42**, 11 356 (2003).
[11] S. Atasayar, H. Gürer-Orhan, H. Orhan, B. Gürel, G. Girgin, H. Özgünes. *Exp. Toxicol. Pathol.*, **61**, 23 (2009).
[12] T. Taguchi, M. Sugiura, Y. Hamada, I. Miwa. *Biochem. Pharm.*, **55**, 1667 (1998).
[13] T. Taguchi, M. Sugiura, Y. Hamada, I. Miwa. *Eur. J. Pharmacol.*, **378**, 283 (1999).
[14] H. Miyoshi, T. Taguchi, M. Sugiura, M. Takeuchi, K. Yanagisawa, Y. Watanable, I. Miwa, Z. Makita, T. Koike. *Horm. Metab. Res.*, **34**, 371 (2002).
[15] A.S. Chen, T. Taguchi, M. Sugiura, Y. Wakasugi, A. Kamei, M.W. Wang, I. Miwa. *Horm. Metab. Res.*, **36**, 183 (2004).
[16] V.M. Leovac, M.D. Joksović, V. Divjaković, Lj.S. Jovanović, Ž. Šaranović, A. Pevec. *J. Inorg. Biochem.*, **101**, 1094 (2007).
[17] V.M. Leovac, Lj.S. Vojinović-Ješić, V.I. Češljević, S.B. Novaković, G.A. Bogdanović. *Acta Cryst.*, **C65**, m337 (2009).
[18] M.M. Lalović, Lj.S. Vojinović-Ješić, Lj.S. Jovanović, V.M. Leovac, V.I. Češljević, V. Divjaković. *Inorg. Chim. Acta*, **388**, 157 (2012).
[19] A. Altomare, G. Cascarano, C. Giacovazzo, A. Gualardi. *J. Appl. Cryst.*, **26**, 343 (1993).
[20] G.M. Sheldrick. *Acta. Cryst.*, **A64**, 112 (2008).
[21] L.J. Farrugia. *J. Appl. Cryst.*, **32**, 837 (1999).
[22] A.L. Spek. *Acta Cryst.*, **D65**, 148 (2009).
[23] W.J. Geary. *Coord. Chem. Rev.*, **7**, 81 (1971).
[24] N. Nakamoto. *Infrared and Raman Spectra of Inorganic and Coordination Compounds*, Wiley, New York (1997).
[25] J. Valdés-Martinez, J.H. Alstrum-Acevedo, R.A. Toscano, S. Hernández-Ortega, G. Espinosa-Pérez, D.X. West, B. Helfrich. *Polyhedron*, **21**, 409 (2002).
[26] A.B.P. Lever. *Inorganic Electronic Spectroscopy* (Russian transl), part 2, pp. 80–90, Mir, Moscow (1987).
[27] T.L. Brown, H.E. LeMay Jr, B.E. Bursten. *Chemistry The Central Science*, Upper Saddle River, New Jersey (2003).
[28] G.E. Bacon, J.S. Plant. *Acta Cryst.*, **B36**, 1130 (1980).
[29] A. Sreekanth, M.R. Prathapachandra Kurup. *Polyhedron*, **23**, 969 (2004).
[30] L. Bjelica, Lj. Jovanović. *J. Electroanal. Chem.*, **213**, 85 (1986).
[31] V.M. Leovac, Lj.S. Jovanović, L.J. Bjelica, V.I. Češljević. *Polyhedron*, **8**, 135 (1989).
[32] V.S. Jevtović, Lj.S. Jovanović, V.M. Leovac, L.J. Bjelica. *J. Serb. Chem. Soc.*, **68**, 929 (2003).
[33] Lj.S. Jovanović. Electrochemical study of iron(III) complexes with semicarbazone-based ligands. PhD thesis, University of Novi Sad (1986) (in Serbian).
[34] M.T. Escot, P. Pouillen, P. Martinet. *Electrochim. Acta*, **26**, 69 (1981).
[35] M.S. Gruzdev, N.E. Domracheva, U.V. Chervonova, A.M. Kolker, A.S. Golubeva. *J. Coord. Chem.*, **65**, 1812 (2012).
[36] M. Sebastian, V. Arun, P.P. Robinson, P. Leeju, G. Varsha, D. Varghese, K.K. Mohammed Yusuff. *J. Coord. Chem.*, **64**, 525 (2011).
[37] R.K. Dubey, U.K. Dubey, S.K. Mishra. *J. Coord. Chem.*, **64**, 2292 (2011).
[38] C.R. Bhattacharjee, P. Goswami, P. Mondal. *J. Coord. Chem.*, **63**, 2002 (2010).